

Quantum many-body attractors

Berislav Buča,^{1,*} Archak Purkayastha,² Giacomo Guarnieri,² Mark T. Mitchison,² Dieter Jaksch,¹ and John Goold²

¹Clarendon Laboratory, University of Oxford, Parks Road, Oxford OX1 3PU, United Kingdom

²School of Physics, Trinity College Dublin, College Green, Dublin 2, Ireland

(Dated: October 2, 2020)

The late P. W. Anderson, in his influential essay ‘More is different’ [1], discussed the importance of broken symmetry for the emergence of fundamental physical laws. Time periodicity is one such symmetry-breaking phenomenon, which Anderson remarked “is either universal or surprisingly common”. One way of understanding the ubiquity of broken time-translation symmetry in complex systems is through non-linearity. Non-linearity in the equations of motion governing a dynamical system is well known to lead to emergent periodic phenomena. A particularly dramatic example of such behaviour in classical physics is an attractor [2]. Here a system may show robust non-stationary dynamics at long times within a restricted manifold of phase space, without fine-tuning of its initial conditions. Such a dynamical state can describe diverse scenarios, including electrical circuits [3], predator-prey communities [4], and the stock market [5]. In quantum systems, however, the Schrödinger equation enforces unitary evolution, intrinsic uncertainty obscures the phase space approach, and entanglement and coherence come to the fore. How, then, can attractors, which are seen in such a diverse range of classical nonlinear systems, arise from the underlying unitary, linear dynamics synonymous with quantum mechanics? Here we show that attractors can appear in a many-body quantum system without a well-defined classical limit, and explain how their existence can be enforced by strictly local dynamical symmetries. The local nature of these dynamical constraints endows the quantum attractor with a remarkable robustness unparalleled in other types of periodic long-time dynamics seen in complex quantum systems.

Periodic long-time dynamics in quantum many-body systems is now under scrutiny in a variety of different scenarios such as time crystals [6–34], models with quantum many-body scars [35–51] and confinement [52–57]. The role of dynamical symmetries [8] in the appearance of periodic dynamics has recently been discussed [9, 58–61], as well as their weaker versions [45–48, 50]. The periodicity of these systems is typically explained from a spectral perspective and is often fragile to variations of the initial state or the Hamiltonian. This is where the attractor that we explicitly construct differs. We will

show that, in systems with an extensive set of dynamical constraints, certain observables do not fully relax but instead display persistent, non-stationary dynamics that does not depend on fine-tuned Hamiltonian parameters or initial conditions. Interestingly, these systems may also have local observables that relax fully to stationarity. Generic observables, which have finite overlap with both non-stationary and relaxing operators, enter a robust orbit that we term a *quantum many-body attractor*. Such behaviour is one of the hallmarks of complex attractive long-time dynamics found in Nature, and sits in stark contrast with both the equilibration behaviour expected for generic quantum many-body systems [62] and the simple persistent oscillations set by the initial value seen in isolated few-body quantum systems. Since the attractor’s properties originate from symmetry, they are preserved at any finite temperature and are exceptionally stable to local modifications of the system Hamiltonian.

We begin by considering a very general scenario: a quantum many-body system on an arbitrary lattice in which every site is connected to the rest of the system. A dynamical symmetry is the property $[\hat{H}, \hat{A}] = -\omega_A \hat{A}$, which defines an eigenoperator \hat{A} of the Hamiltonian \hat{H} . Given an out of equilibrium initial state $\hat{\rho}$, i.e. $[\hat{\rho}, \hat{H}] \neq 0$, the expectation value of \hat{A} oscillates periodically in time as $\langle \hat{A}(t) \rangle = e^{-i\omega_A t} \langle \hat{A}(0) \rangle$. An exponentially large set of such eigenoperators can always trivially be found, yet generally such quantities are highly non-local operators that are inaccessible to local measurements in a large system.

The situation becomes non-trivial when there exists an eigenoperator \hat{A} that is *strictly local*, i.e. supported on only a few neighbouring lattice sites. We can then divide the system into two parts, such that $\hat{H} = \hat{H}_A + \hat{H}'_A$ with

$$[\hat{H}_A, \hat{A}] = -\omega_A \hat{A}, \quad [\hat{H}'_A, \hat{A}] = 0, \quad (1)$$

while $[\hat{H}_A, \hat{H}'_A] \neq 0$ in general. Here, \hat{H}_A is a Hamiltonian defined on a few contiguous sites of the lattice, such that its support is strictly larger than that of \hat{A} (see Fig. 1(a)). That is, the support of \hat{A} does not include the boundary of the support of \hat{H}_A . Meanwhile, \hat{H}'_A shares the boundary of its support with \hat{H}_A and also covers the rest of the lattice. As a result, the persistent oscillations associated with \hat{A} are protected from any change in \hat{H}'_A . Furthermore, it can be easily checked that $\hat{Q} = [\hat{A}^\dagger, \hat{A}]$ is a strictly local conserved quantity of the system, i.e. $[\hat{H}, \hat{Q}] = [\hat{H}_A, \hat{Q}] = 0$. Eq. (1) gives a quadratic set of

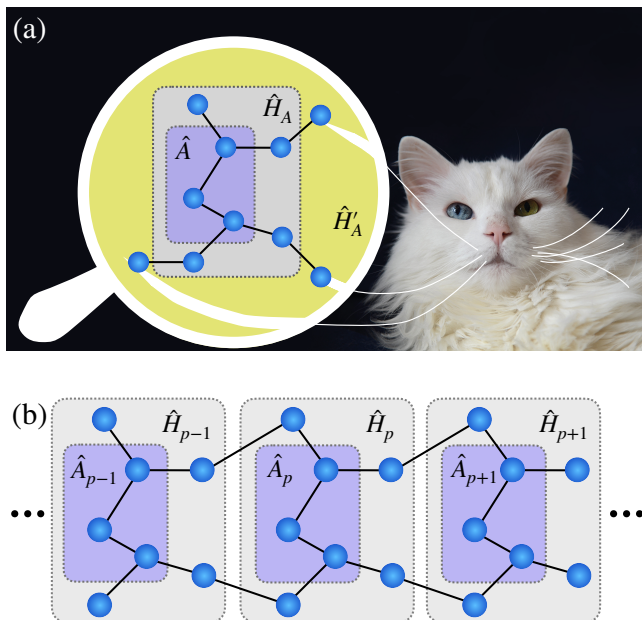


FIG. 1. **Constructing a many-body system with strictly local dynamical symmetries.** (a) Schematic close-up of an arbitrary lattice showing the supports of a strictly local dynamical symmetry \hat{A} and its associated local Hamiltonian \hat{H}_A . The remainder of the system can be governed by any Hamiltonian \hat{H}'_A without affecting the local dynamical symmetry. (b) Connecting local Hamiltonians together as shown builds a many-body system with an extensive number of strictly local dynamical symmetries.

equations that may be solved to generate a candidate \hat{H}_A and \hat{A} provided that we demand it holds for any \hat{H}'_A .

Since \hat{A} is not supported on the boundary of \hat{H}_A , we can connect several of these local Hamiltonians via their boundary sites without disrupting the dynamical symmetry (see Fig. 1(b)). The full Hamiltonian of such a system can be written as a sum of strictly local Hamiltonians $\hat{H} = \sum_p \hat{H}_p$, each \hat{H}_p being associated with its own strictly local dynamical symmetry \hat{A}_p , i.e. $[\hat{H}_p, \hat{A}_q] = -\omega_q \hat{A}_q \delta_{pq}$, with δ_{pq} the Kronecker delta symbol. This many-body system has an extensive number of strictly local operators that persistently oscillate at frequency ω_q and never relax to a stationary value. Crucially, moreover, the connectivity of the lattice implies that $[\hat{H}_p, \hat{H}_{p+1}] \neq 0$. As shown below, this allows local observables that overlap with \hat{A}_p to undergo partial relaxation and tend to a limit cycle at long times. A system may have multiple, possibly incommensurate, frequencies ω_q and the orbit to which the observables converge can form more complicated structures than a limit cycle.

Even if the initial state is stationary, i.e. $[\hat{\rho}, \hat{H}] = 0$, an arbitrarily small perturbation will initiate persistent oscillations. This can be understood as a manifestation of spontaneously broken (continuous) time-translation

symmetry. Consider a small instantaneous perturbation \hat{H}_{pert} applied to a stationary state [63, 64], such that the Hamiltonian is $\hat{H}_{\text{tot}} = \hat{H} + \delta(t)\hat{H}_{\text{pert}}$, with $\delta(t)$ the Dirac delta function. According to linear-response theory, the resulting change in an observable \hat{O} is $\delta O(t) = \langle \hat{O}_{\text{tot}}(t) \rangle - \langle \hat{O}(0) \rangle = -i\langle [\hat{O}(t), \hat{H}_{\text{pert}}] \rangle$, where $\hat{O}_{\text{tot}}(t) = e^{i\hat{H}_{\text{tot}}t}\hat{O}e^{-i\hat{H}_{\text{tot}}t}$ and $\hat{O}(t) = e^{i\hat{H}t}\hat{O}e^{-i\hat{H}t}$.

Within this framework, we can distinguish three fundamentally different kinds of response. A dynamical symmetry operator \hat{A}_p shows persistent oscillations, since

$$\delta A_p(t) = -ie^{-i\omega_p t} \langle [\hat{A}_p, \hat{H}_{\text{pert}}] \rangle. \quad (2)$$

In contrast, a local conserved charge $\hat{Q}_p = [\hat{A}_p^\dagger, \hat{A}_p]$ has a response that is constant in time, i.e. $\delta Q_p(t) = -i\langle [\hat{Q}_p, \hat{H}_{\text{pert}}] \rangle$. In addition, there may exist local observables \hat{O} that do not overlap with either the dynamical symmetry operators or the associated conserved charges, in the sense that $\langle \hat{O}\hat{A}_p \rangle = \langle \hat{O}\hat{Q}_p \rangle = 0$. In the absence of further conservation laws, the response of such an observable relaxes to zero, $\lim_{t \rightarrow \infty} \delta O(t) = 0$. This returns the observable to its original expectation value, thus losing all memory of the perturbation.

As we show below, all three kinds of dynamics may robustly coexist in an interacting quantum many-body system with strictly local dynamical symmetries. In particular, a generic observable that overlaps with the \hat{A}_p will partially lose memory of the initial perturbation while also inheriting the oscillatory behaviour of Eq. (2). As a result, the system retains complex dynamics in the long-time limit within a restricted manifold of the “phase space” spanned by local observables. Such stable orbits are largely independent of the initial conditions and thus correspond to a quantum many-body attractor.

Although this attractor spontaneously breaks time-translation symmetry, it does not conform to the definition of a continuous time crystal put forward in Ref. [65] because it violates a particular condition for spatial long-range order that is designed to exclude non-interacting systems. Nevertheless, the existence of observables that lose memory of their initial conditions — a typical characteristic of an interacting system — explicitly distinguishes our setup from a trivial collection of disconnected subsystems. However, it is important to note that the extensive set of conserved charges \hat{Q}_p makes the models generated through our approach quasi-integrable [62, 66]. Despite this, the stability of such models is quite unlike standard quantum integrability [67–70]. In particular, arbitrarily changing any local Hamiltonian \hat{H}_p can, at worst, destroy the local symmetry \hat{A}_p associated with it, leaving all others unaffected.

We now construct an explicit spin lattice model showing quantum many-body attractor dynamics. The unit cell of the lattice comprises three sites, each corresponding to a spin-half degree of freedom, which are sewn together to form the “spin lace” structure depicted in

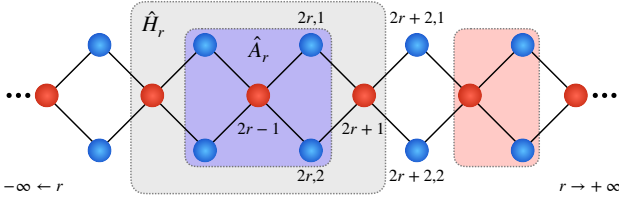


FIG. 2. **Spin-lace model.** Each unit cell (red box) comprises three lattice sites occupied by a spin-half. Spins in the r^{th} unit cell are described by standard Pauli operators, denoted by $\hat{\sigma}_{2r-1}^\alpha$ for the inner (red) site and $\hat{\sigma}_{2r,1}^\alpha$ or $\hat{\sigma}_{2r,2}^\alpha$ for the outer (blue) sites, with $\alpha = x, y, z$. The spin operators appearing in the Hamiltonian (3) are then $\hat{s}_r^\alpha = \hat{\sigma}_{2r-1}^\alpha$ and $\hat{S}_r^\alpha = \hat{\sigma}_{2r,1}^\alpha + \hat{\sigma}_{2r,2}^\alpha$. The operator \hat{A}_r is defined in Eq. (4) via the singlet projectors $\hat{P}_r = |\psi_-\rangle_r \langle \psi_-|$, where $|\psi_-\rangle_r \propto |\uparrow\rangle_{2r,1} |\downarrow\rangle_{2r,2} - |\downarrow\rangle_{2r,1} |\uparrow\rangle_{2r,2}$, leading to a local dynamical symmetry supported on five lattice sites (purple box). These sites are embedded in a seven-site plaquette (grey box) governed by the strictly local Hamiltonian $\hat{H}_r = \hat{h}_r + B_{r-1} \hat{S}_{r-1}^z + \frac{1}{2} (b_{r+1} \hat{s}_{r+1}^z + b_{r-1} \hat{s}_{r-1}^z) + \sum_\alpha (J_{\alpha,r-1} \hat{s}_{r-1}^\alpha \hat{S}_{r-1}^\alpha + J'_{\alpha,r+1} \hat{s}_{r+1}^\alpha \hat{S}_r^\alpha)$, such that the total Hamiltonian reads $\hat{H} = \sum_p \hat{H}_{2p-1}$.

Fig. 2. The Hamiltonian can be written as $\hat{H} = \sum_r \hat{h}_r$, where r labels the unit cells and

$$\hat{h}_r = b_r \hat{s}_r^z + B_r \hat{S}_r^z + \sum_{\alpha=x,y,z} \left(J_r^\alpha \hat{s}_r^\alpha \hat{S}_r^\alpha + K_r^\alpha \hat{s}_r^\alpha \hat{S}_{r-1}^\alpha \right). \quad (3)$$

Here, b_r and B_r are local magnetic fields, $J_r^{x,y,z}$ and $K_r^{x,y,z}$ are respectively the exchange couplings within and between unit cells, \hat{s}_r^α are spin operators for the inner (red) site, and \hat{S}_r^α are operators describing the *total* spin of the outer (blue) pair of sites in each unit cell. The appearance of the total spin \hat{S}_r^α in Eq. (3) is due to the up-down permutation invariance of the spin lace, which implies the existence of strictly local dynamical symmetry operators

$$\hat{A}_r = \hat{P}_{r-1} \hat{s}_r \hat{P}_r \Rightarrow [\hat{H}_r, \hat{A}_{r'}] = -2b_r \hat{A}_r \delta_{rr'}. \quad (4)$$

Here, \hat{P}_r is the projector onto the singlet subspace satisfying $\hat{S}_r^\alpha \hat{P}_r = \hat{P}_r \hat{S}_r^\alpha = 0$, while \hat{H}_r is one of the associated strictly local Hamiltonians, which partition the spin lace into overlapping plaquettes such that $\hat{H} = \sum_p \hat{H}_{2p-1}$; see Fig. 2 for details. The strictly local dynamical symmetries are preserved for arbitrary spatial variations of the local fields and exchange couplings in Eq. (3). Furthermore, local modifications of \hat{h}_r that violate the up-down permutation symmetry only affect nearby plaquettes, leaving the dynamical symmetries throughout the rest of the system unchanged.

From here on, we focus on the homogeneous spin lace with $b_r = B_r = B$ and $J_r^\alpha = K_r^\alpha = J^\alpha$. In Fig. 3(a) we calculate the time evolution of several correlation functions at infinite temperature. Observables having finite overlap with the dynamical symmetry operators show

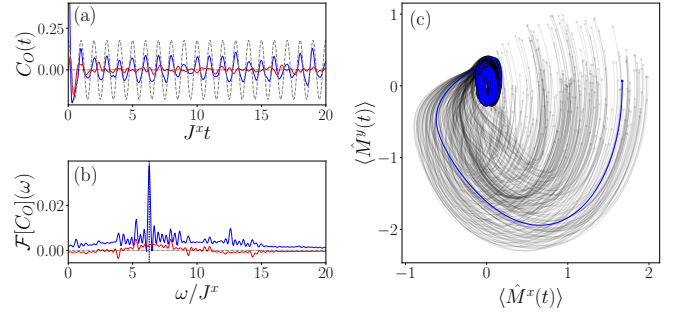


FIG. 3. **Quantum many-body attractor in the homogeneous spin lace.** (a) Infinite-temperature correlation functions $C_O(t) = \langle \hat{O}(t) \hat{s}_r^x \rangle$, describing the linear response of the observable $\hat{O}(t)$ to a local perturbation $\hat{H}_{\text{pert}} \propto \hat{s}_r^x$ applied to one lattice site. Persistent oscillations are seen for observables which overlap with a dynamical symmetry operator, such as \hat{s}_r^x (blue solid lines) or \hat{A}_r (gray dotted line) itself. In contrast, the response of non-conserved observables, e.g. the total spin operator \hat{S}_r^x (red solid lines), decays to small fluctuations around zero, showing complete loss of memory of initial conditions. (b) Fourier transforms $\mathcal{F}[C_O(t)](\omega)$ of the correlation functions shown in (a). The dominant frequency $\omega = 2B$ (vertical dashed line) is clear in the response of \hat{s}_r^x , while the response of \hat{S}_r^x shows no special feature at that frequency. (c) Attractive dynamics of the total magnetisation vector $\hat{M}^\alpha = L^{-1} \sum_r (\hat{s}_r^\alpha + \hat{S}_r^\alpha)$ in the x - y plane, where L is the number of lattice sites. Each line shows an evolution that starts from a different initial condition and is drawn over time into a complex orbit within the attractor region. The attractor is visible as the shaded ellipse where all spin trajectories converge. The blue line highlights one representative trajectory. The initial conditions are generated by preparing the system in an infinite-temperature state and then projecting the total spin state of all unit cells in a given direction. See the Methods for details. Parameters: $J^x = 1, J^y = 2, J^z = 0.5, B = \pi$.

persistent oscillations, indicating broken time-translation symmetry. Conversely, observables proportional to the total spin operators \hat{S}_r^α relax back to their equilibrium value, up to small fluctuations that we attribute to numerical finite-size effects. The disparity between these two behaviours is clearly seen in the Fourier domain (Fig. 3(b)), where a dominant peak at frequency $2B$ distinguishes oscillatory observables from relaxing ones. It is notable that the microscopic frequency $2B$ — a property of the local Hamiltonian (3) — remains a perfectly preserved spectral feature even in an interacting many-body system.

The combination of oscillatory and relaxing dynamics leads generic observables to converge to a non-trivial attractor. We demonstrate this in Fig. 3(c), which shows the evolution of the total magnetisation starting from various different global spin orientations. For all initial conditions considered, this macroscopic observable is drawn towards the same restricted volume of its configuration space, where it follows complex, non-stationary

orbits that persist in the long-time limit. Similar behaviour would be seen even if the Hamiltonian is locally modified in one portion of the system, or if the exchange couplings differ throughout the lattice. The insensitivity of the attractor to variations of both the starting configuration and the microscopic system parameters is a hallmark of the attractors familiar from classical physics. However, due to its low-dimensional geometry and finite local Hilbert spaces, the spin lace is inherently resistant to quasi-classical descriptions, e.g. mean-field approximations or semi-classical limits. Therefore, the quantum many-body attractor cannot solely be understood as an emergent classical phenomenon, but instead is a direct consequence of local dynamical symmetry constraints on the quantum-mechanical equations of motion.

The quantum many-body attractor is a dynamical state of matter in which oscillatory behaviour conspires with relaxation to yield robust, complex dynamics that is reminiscent of classical non-linear systems. In this work, we have explicitly constructed a theoretical model of a quantum many-body attractor with strictly local dynamical symmetries. We postulate that such attractors may appear naturally in strongly interacting quantum many-body systems with a similar structure. These include magnetic materials with tetramer unit cells [71–73] and diamond lattice compounds much studied for their interesting low-temperature properties [74–80]. Indeed, local dynamical symmetries in complex systems may well be behind the ubiquitous temporal regularity in Nature that Anderson discussed almost half a century ago [1].

Acknowledgements — BB warmly acknowledges V. Jukić Buča for the name “spin lace” and help with Fig 1a containing Pulci. BB thanks M. Medenjak for useful discussions and collaboration on related work, H. Katsura for critical reading and valuable corrections and O. Castro Alvaredo, B. Doyon, J. Marino, C. Navarrete-Benlloch, A. Polkovnikov, F. Pollmann, and T. Prosen for useful discussions. We acknowledge support from the European Research Council Starting Grant ODYSSEY (G. A. 758403). JG would like to thank A. Silva and M. Dalmonte for discussions. BB and DJ acknowledge funding from EPSRC programme grant EP/P009565/1, EPSRC National Quantum Technology Hub in Networked Quantum Information Technology (EP/M013243/1), and the European Research Council under the European Union’s Seventh Framework Programme (FP7/2007-2013)/ERC Grant Agreement no. 319286, Q-MAC. JG is supported by a SFI-Royal Society University Research Fellowship. AP acknowledges funding from European Unions Horizon 2020 research and innovation programme under the Marie Skłodowska-Curie grant agreement No. 890884. AP acknowledges Irish Centre for High End Computing (ICHEC) for the provision of computational facilities.

METHODS

Infinite temperature correlation functions with tensor networks

For a spin system with L lattice sites, the infinite temperature two-time correlation function between two operators \hat{O}_1 and \hat{O}_2 is given by $\frac{1}{2^L} \text{Tr}(\hat{O}_2 e^{i\hat{H}t} \hat{O}_1 e^{-i\hat{H}t})$. Going to a super-operator representation, this can be written as $\frac{1}{2^L} \langle \hat{O}_2 | e^{i\hat{H}t} \otimes e^{-i\hat{H}t} | \hat{O}_1 \rangle$. For (quasi) one-dimensional systems, by trotterizing the time evolution and using a matrix-product-state (MPS) representation of $|\hat{O}_1\rangle$ and $|\hat{O}_2\rangle$, this can be efficiently calculated via a standard time-evolution-by-block-decimation (TEBD) approach [81]. The correlation functions can be obtained for very large system sizes, but up to a finite time, due to a finite bond dimension used in the tensor networks. In our numerical simulation for Fig. 3(a), we considered a spin lace of 100 unit cells (300 sites), which models the system essentially in the thermodynamic limit for the time scales simulated. The maximum bond dimension used was 200 which allowed accurate simulation up to time $t = 20$ in units of J_x .

The frequency response from the correlation functions

The frequency response shown in Fig. 3(b) is numerically obtained from the finite-time evolution data in Fig. 3(a) by calculating the function

$$\mathcal{F}[C_O](\omega) = \frac{1}{T} \int_0^T dt e^{i\omega t} C_O(t), \quad (5)$$

where T is the maximum simulation time and $C_O(t) = \langle \hat{O}(t) \hat{s}_r^x \rangle$ is the correlation function describing the response of \hat{O} to a perturbation $\hat{H}_{\text{pert}} \propto \hat{s}_r^x$.

Generation of initial states

In Fig. 3(c) we demonstrate the convergence of local observables to a non-stationary quantum many-body attractor starting from different initial conditions. Specifically, we consider global magnetisation configurations that correspond to initial preparations of the product form $\hat{\rho} = \bigotimes_r \hat{\rho}_r$, with $\hat{\rho}_r$ the local state describing one unit cell. For concreteness, we take

$$\hat{\rho}_r = \frac{1}{8} \left(\hat{\mathbb{I}}_2 + \hat{\sigma}_{2r-1}^x \right) \otimes \left(\mathbb{I}_2 + a\hat{\sigma}_{2r,1}^x + b\hat{\sigma}_{2r,1}^y + c\hat{\sigma}_{2r,1}^z \right) \otimes \left(\hat{\mathbb{I}}_2 \right), \quad (6)$$

where $\hat{\mathbb{I}}_2$ is the 2×2 identity operator and $\{a, b, c\}$ are uniform random numbers in $[-1, 1]$ such that

$\sqrt{a^2 + b^2 + c^2} = 1$. This describes an infinite-temperature state that is perturbed by projecting the spin at each inner (red, $2r - 1$) site onto the positive x direction and the neighbouring spin at the top site (blue, $2r, 1$) in the same random direction. Due to the strict locality of the dynamical symmetries and the translation invariance of the lattice, it is sufficient to project a single cell r in this way, i.e. to take an initial state $\hat{\rho} = \hat{\rho}_r \otimes_{r' \neq r} \hat{I}_2^{\otimes 3}$, and then compute the subsequent evolution of local observables within cell r . Summing the results over all cells in the lattice, we obtain Fig. 3(c). The resulting attractor dynamics can be shown to be identical to that obtained from a translation-invariant initial state of the form $\hat{\rho} = \otimes_r \hat{\rho}_r$, as correlations between different unit cells decay rapidly with the distance between them and do not contribute asymptotically.

* berislav.buca@physics.ox.ac.uk

- [1] P. W. Anderson, “More Is Different,” *Science* **177**, 393–396 (1972).
- [2] Predrag Cvitanovic, Roberto Artuso, Ronnie Mainieri, Gregor Tanner, Gábor Vattay, Niall Whelan, and Andreas Wirzba, “Chaos: classical and quantum,” *Chaos-Book.org* (Niels Bohr Institute, Copenhagen 2005) (2005).
- [3] Louis M. Pecora and Thomas L. Carroll, “Synchronization in chaotic systems,” *Phys. Rev. Lett.* **64**, 821–824 (1990).
- [4] Sergio Rinaldi, Simona Muratori, and Yuri Kuznetsov, “Multiple attractors, catastrophes and chaos in seasonally perturbed predator-prey communities,” *Bull. Math. Biol.* **55**, 15–35 (1993).
- [5] Edgar E. Peters, “A Chaotic Attractor for the S&P 500,” *FAJ* **47**, 55–81 (1991).
- [6] Frank Wilczek, “Quantum Time Crystals,” *Phys. Rev. Lett.* **109**, 160401 (2012).
- [7] Dominic V. Else, Christopher Monroe, Chetan Nayak, and Norman Y. Yao, “Discrete Time Crystals,” *Annu. Rev. Condens. Matter Phys.* **11**, 467–499 (2020).
- [8] Berislav Buča, Joseph Tindall, and Dieter Jaksch, “Non-stationary coherent quantum many-body dynamics through dissipation,” *Nat. Comm.* **10**, 1730 (2019).
- [9] Marko Medenjak, Berislav Buča, and Dieter Jaksch, “Isolated Heisenberg magnet as a quantum time crystal,” *Phys. Rev. B* **102**, 041117 (2020).
- [10] Vedika Khemani, Achilleas Lazarides, Roderich Moessner, and S. L. Sondhi, “Phase Structure of Driven Quantum Systems,” *Phys. Rev. Lett.* **116**, 250401 (2016).
- [11] Dominic V. Else, Bela Bauer, and Chetan Nayak, “Floquet time crystals,” *Phys. Rev. Lett.* **117**, 090402 (2016).
- [12] Achilleas Lazarides, Arnab Das, and Roderich Moessner, “Periodic thermodynamics of isolated quantum systems,” *Phys. Rev. Lett.* **112**, 150401 (2014).
- [13] Pranjal Bordia, Henrik Lüschen, Ulrich Schneider, Michael Knap, and Immanuel Bloch, “Periodically driving a many-body localized quantum system,” *Nat. Phys.* **13**, 460 (2017).
- [14] Wing Chi Yu, Jirawat Tangpanitanon, Alexander W. Glaetzle, Dieter Jaksch, and Dimitris G. Angelakis, “Discrete time crystal in globally driven interacting quantum systems without disorder,” *Phys. Rev. A* **99**, 033618 (2019).
- [15] Bihui Zhu, Jamir Marino, Norman Y Yao, Mikhail D Lukin, and Eugene A Demler, “Dicke time crystals in driven-dissipative quantum many-body systems,” *New J. Phys.* **21**, 073028 (2019).
- [16] F. M. Gambetta, F. Carollo, A. Lazarides, I. Lesanovsky, and J. P. Garrahan, “Classical stochastic discrete time crystals,” *Phys. Rev. E* **100** (2019).
- [17] Krzysztof Giergiel, Alexandre Dauphin, Maciej Lewenstein, Jakub Zakrzewski, and Krzysztof Sacha, “Topological time crystals,” *New J. Phys.* **21**, 052003 (2019).
- [18] F. M. Gambetta, F. Carollo, M. Marcuzzi, J. P. Garrahan, and I. Lesanovsky, “Discrete time crystals in the absence of manifest symmetries or disorder in open quantum systems,” *Phys. Rev. Lett.* **122**, 015701 (2019).
- [19] D. A. Ivanov, T. Yu. Ivanova, S. F. Caballero-Benitez, and I. B. Mekhov, “Feedback-induced quantum phase transitions using weak measurements,” *Phys. Rev. Lett.* **124**, 010603 (2020).
- [20] Guido Homann, Jayson G. Cosme, and Ludwig Mathey, “Higgs Time Crystal in a High- T_c Superconductor,” (2020), [arXiv:2004.13383 \[cond-mat.supr-con\]](https://arxiv.org/abs/2004.13383).
- [21] Reuben R. W. Wang, Bo Xing, Gabriel G. Carlo, and Dario Poletti, “Period doubling in period-one steady states,” *Phys. Rev. E* **97**, 020202 (2018).
- [22] Nishant Dogra, Manuele Landini, Katrin Kroeger, Lorenz Hruby, Tobias Donner, and Tilman Esslinger, “Dissipation induced structural instability and chiral dynamics in a quantum gas,” *arXiv preprint arXiv:1901.05974* (2019).
- [23] E. I. Rodríguez Chiacchio and A. Nunnenkamp, “Dissipation-induced instabilities of a spinor bose-einstein condensate inside an optical cavity,” *Phys. Rev. Lett.* **122**, 193605 (2019).
- [24] Diego Barberena, Robert J. Lewis-Swan, James K. Thompson, and Ana Maria Rey, “Driven-dissipative quantum dynamics in ultra-long-lived dipoles in an optical cavity,” *Phys. Rev. A* **99**, 053411 (2019).
- [25] C. Lledó, Th. K. Mavrogordatos, and M. H. Szymańska, “Driven Bose-Hubbard dimer under nonlocal dissipation: A bistable time crystal,” *Phys. Rev. B* **100**, 054303 (2019).
- [26] Jayson G. Cosme, Jim Skulte, and Ludwig Mathey, “Time crystals in a shaken atom-cavity system,” *Phys. Rev. A* **100**, 053615 (2019).
- [27] Kilian Seibold, Riccardo Rota, and Vincenzo Savona, “Dissipative time crystal in an asymmetric nonlinear photonic dimer,” *Phys. Rev. A* **101**, 033839 (2020).
- [28] Andreu Riera-Campenya, Maria Moreno-Cardoner, and Anna Sanpera, “Time crystallinity in open quantum systems,” (2019), [arXiv:1908.11339 \[quant-ph\]](https://arxiv.org/abs/1908.11339).
- [29] Hans Keßler, Jayson G. Cosme, Michal Hemmerling, Ludwig Mathey, and Andreas Hemmerich, “Emergent limit cycles and time crystal dynamics in an atom-cavity system,” *Phys. Rev. A* **99**, 053605 (2019).
- [30] Orazio Scarlatella, Rosario Fazio, and Marco Schiró, “Emergent finite frequency criticality of driven-dissipative correlated lattice bosons,” *Phys. Rev. B* **99**, 064511 (2019).

- [31] Hans Keler, Jayson G. Cosme, Christoph Georges, Ludwig Mathey, and Andreas Hemmerich, “From a continuous to a discrete time crystal,” (2020), [arXiv:2004.14633 \[cond-mat.quant-gas\]](#).
- [32] Fabrizio Minganti, Ievgen I. Arkhipov, Adam Miranowicz, and Franco Nori, “Correspondence between dissipative phase transitions of light and time crystals,” (2020), [arXiv:2008.08075 \[quant-ph\]](#).
- [33] Ching-Kit Chan, Tony E. Lee, and Sarang Gopalakrishnan, “Limit-cycle phase in driven-dissipative spin systems,” *Phys. Rev. A* **91**, 051601 (2015).
- [34] Vladimir Gritsev and Anatoli Polkovnikov, “Integrable Floquet dynamics,” *SciPost Physics* **2** (2017).
- [35] C. J. Turner, A. A. Michailidis, D. A. Abanin, M. Serbyn, and Z. Papić, “Weak ergodicity breaking from quantum many-body scars,” *Nat. Phys.* **14**, 745–749 (2018).
- [36] Sanjay Moudgalya, Stephan Rachel, B. Andrei Bernevig, and Nicolas Regnault, “Exact excited states of nonintegrable models,” *Phys. Rev. B* **98** (2018).
- [37] Soonwon Choi, Christopher J. Turner, Hannes Pichler, Wen Wei Ho, Alexios A. Michailidis, Zlatko Papić, Maksym Serbyn, Mikhail D. Lukin, and Dmitry A. Abanin, “Emergent SU(2) Dynamics and Perfect Quantum Many-Body Scars,” *Phys. Rev. Lett.* **122**, 220603 (2019).
- [38] Cheng-Ju Lin and Olexei I. Motrunich, “Exact Quantum Many-Body Scar States in the Rydberg-Blockaded Atom Chain,” *Phys. Rev. Lett.* **122**, 173401 (2019).
- [39] Thomas Iadecola and Michael Schechter, “Quantum many-body scar states with emergent kinetic constraints and finite-entanglement revivals,” *Phys. Rev. B* **101** (2020).
- [40] Sanjay Moudgalya, Nicolas Regnault, and B. Andrei Bernevig, “Entanglement of exact excited states of Affleck-Kennedy-Lieb-Tasaki models: Exact results, many-body scars, and violation of the strong eigenstate thermalization hypothesis,” *Phys. Rev. B* **98** (2018).
- [41] Christopher J. Turner, Jean-Yves Desaulles, Kieran Bull, and Zlatko Papi, “Correspondence principle for many-body scars in ultracold Rydberg atoms,” (2020), [arXiv:2006.13207 \[quant-ph\]](#).
- [42] Michael Schechter and Thomas Iadecola, “Weak Ergodicity Breaking and Quantum Many-Body Scars in Spin-1 XY Magnets,” *Phys. Rev. Lett.* **123** (2019).
- [43] A. A. Michailidis, C. J. Turner, Z. Papi, D. A. Abanin, and M. Serbyn, “Stabilizing two-dimensional quantum scars by deformation and synchronization,” *Phys. Rev. Res.* **2** (2020).
- [44] Hannes Bernien, Sylvain Schwartz, Alexander Keesling, Harry Levine, Ahmed Omran, Hannes Pichler, Soonwon Choi, Alexander S. Zibrov, Manuel Endres, Markus Greiner, Vladan Vuletić, and Mikhail D. Lukin, “Probing many-body dynamics on a 51-atom quantum simulator,” *Nature* **551**, 579 EP – (2017).
- [45] Kieran Bull, Jean-Yves Desaulles, and Zlatko Papi, “Quantum scars as embeddings of weakly broken Lie algebra representations,” *Phys. Rev. B* **101** (2020).
- [46] Sanjay Moudgalya, Nicolas Regnault, and B. Andrei Bernevig, “Eta-Pairing in Hubbard Models: From Spectrum Generating Algebras to Quantum Many-Body Scars,” (2020), [arXiv:2004.13727 \[cond-mat.str-el\]](#).
- [47] Daniel K. Mark and Olexei I. Motrunich, “Eta-pairing states as true scars in an extended Hubbard Model,” (2020), [arXiv:2004.13800 \[cond-mat.str-el\]](#).
- [48] Daniel K. Mark, Cheng-Ju Lin, and Olexei I. Motrunich, “Unified structure for exact towers of scar states in the Affleck-Kennedy-Lieb-Tasaki and other models,” *Phys. Rev. B* **101** (2020).
- [49] Kiryl Pakrouski, Preethi N. Pallegar, Fedor K. Popov, and Igor R. Klebanov, “Many Body Scars as a Group Invariant Sector of Hilbert Space,” (2020), [arXiv:2007.00845 \[cond-mat.str-el\]](#).
- [50] Nicholas O’Dea, Fiona Burnell, Anushya Chandran, and Vedika Khemani, “From tunnels to towers: quantum scars from Lie Algebras and q-deformed Lie Algebras,” (2020), [arXiv:2007.16207 \[cond-mat.stat-mech\]](#).
- [51] Naoyuki Shibata, Nobuyuki Yoshioka, and Hosho Katsura, “Onsager’s scars in disordered spin chains,” *Phys. Rev. Lett.* **124**, 180604 (2020).
- [52] Alessio Lerose, Federica M. Surace, Paolo P. Mazza, Gabriele Perfetto, Mario Collura, and Andrea Gambassi, “Quasiloclized dynamics from confinement of quantum excitations,” *Phys. Rev. B* **102**, 041118 (2020).
- [53] Axel Corts Cubero and Neil J. Robinson, “Lack of thermalization in (1+1)-d QCD at large N_c ,” (2019), [arXiv:1908.00270 \[hep-th\]](#).
- [54] Shriya Pai and Michael Pretko, “Fractons from confinement in one dimension,” *Phys. Rev. Res.* **2** (2020).
- [55] Marton Kormos, Mario Collura, Gabor Takacs, and Pasquale Calabrese, “Real-time confinement following a quantum quench to a non-integrable model,” *Nat. Phys.* **13**, 246 (2016).
- [56] Neil J. Robinson, Andrew J. A. James, and Robert M. Konik, “Signatures of rare states and thermalization in a theory with confinement,” *Phys. Rev. B* **99** (2019).
- [57] Olalla A. Castro-Alvaredo, Máté Lencsés, István M. Szécsényi, and Jacopo Viti, “Entanglement oscillations near a quantum critical point,” *Phys. Rev. Lett.* **124**, 230601 (2020).
- [58] Marko Medenjak, Tomaz Prosen, and Lenart Zadnik, “Rigorous bounds on dynamical response functions and time-translation symmetry breaking,” *SciPost Physics* **9** (2020).
- [59] Koki Chinzei and Tatsuhiko N. Ikeda, “Time Crystals Protected by Floquet Dynamical Symmetry in Hubbard Models,” *Phys. Rev. Lett.* **125** (2020).
- [60] Berislav Buča and Dieter Jaksch, “Dissipation induced nonstationarity in a quantum gas,” *Phys. Rev. Lett.* **123**, 260401 (2019).
- [61] J Tindall, C Sánchez Muñoz, B Buča, and D Jaksch, “Quantum synchronisation enabled by dynamical symmetries and dissipation,” *New J. Phys.* **22**, 013026 (2020).
- [62] Luca D’Alessio, Yariv Kafri, Anatoli Polkovnikov, and Marcos Rigol, “From quantum chaos and eigenstate thermalization to statistical mechanics and thermodynamics,” *Adv. Phys.* **65**, 239–362 (2016).
- [63] Gesualdo Delfino, “Quantum quenches with integrable pre-quench dynamics,” *J. Phys. A* **47**, 402001 (2014).
- [64] Gesualdo Delfino, “Persistent oscillations after quantum quenches: The inhomogeneous case,” *Nucl. Phys. B* **954**, 115002 (2020).
- [65] Vedika Khemani, C. W. von Keyserlingk, and S. L. Sondhi, “Defining time crystals via representation theory,” *Phys. Rev. B* **96**, 115127 (2017).
- [66] Maurizio Fagotti, “On conservation laws, relaxation and pre-relaxation after a quantum quench,” *J. Stat. Mech.: Theory Exp* **2014**, P03016 (2014).

- [67] Marlon Brenes, Tyler LeBlond, John Goold, and Marcos Rigol, “Eigenstate thermalization in a locally perturbed integrable system,” *Phys. Rev. Lett.* **125**, 070605 (2020).
- [68] Marko Znidaric, “Weak integrability breaking: chaos with integrability signature in coherent diffusion,” [arXiv preprint arXiv:2006.09793](#) (2020).
- [69] Lea F. Santos, Francisco Pérez-Bernal, and E. Jonathan Torres-Herrera, “Speck of chaos,” [arXiv e-prints](#) (2020), [arXiv:2006.10779](#) [[cond-mat.stat-mech](#)].
- [70] Mohit Pandey, Pieter W. Claeys, David K. Campbell, Anatoli Polkovnikov, and Dries Sels, “Adiabatic eigenstate deformations as a sensitive probe for quantum chaos,” (2020), [arXiv:2004.05043](#) [[quant-ph](#)].
- [71] Michael A. McGuire, V. Ovidiu Garlea, Santosh KC, Valentino R. Cooper, Jiaqiang Yan, Huibo Cao, and Brian C. Sales, “Antiferromagnetism in the van der Waals layered spin-lozenge semiconductor CrTe_3 ,” *Phys. Rev. B* **95**, 144421 (2017).
- [72] M Hagiwara, Y Narumi, A Matsuo, H Yashiro, S Kimura, and K Kindo, “Magnetic properties of a ni tetramer with a butterfly structure in high magnetic fields,” *New J. Phys.* **8**, 176–176 (2006).
- [73] Hiroshi Sakiyama, Masatoshi Kato, Satoshi Sasaki, Moriya Tasaki, Eiji Asato, and Masayuki Koikawa, “Synthesis and magnetic properties of a dinuclear manganese (II) complex with two manganese (II) ions of C₂-twisted octahedral geometry,” *Polyhedron* **111**, 32–37 (2016).
- [74] H. Kikuchi, Y. Fujii, M. Chiba, S. Mitsudo, T. Idehara, T. Tonegawa, K. Okamoto, T. Sakai, T. Kuwai, and H. Ohta, “Experimental Observation of the 1/3 Magnetization Plateau in the Diamond-Chain Compound $\text{Cu}_3(\text{CO}_3)_2(\text{OH})_2$,” *Phys. Rev. Lett.* **94**, 227201 (2005).
- [75] K. C. Rule, A. U. B. Wolter, S. Süllow, D. A. Tennant, A. Brühl, S. Köhler, B. Wolf, M. Lang, and J. Schreuer, “Nature of the Spin Dynamics and 1/3 Magnetization Plateau in Azurite,” *Phys. Rev. Lett.* **100**, 117202 (2008).
- [76] “Static and dynamic magnetic properties of the spin- $\frac{1}{2}$ inequilateral diamond-chain compounds , author = Morita, Katsuhiko and Fujihala, Masayoshi and Koorikawa, Hiroko and Sugimoto, Takanori and Sota, Shigetoshi and Mitsuda, Setsuo and Tohyama, Takami, journal = Phys. Rev. B, volume = 95, issue = 18, pages = 184412, numpages = 5, year = 2017, month = May, publisher = American Physical Society, doi = 10.1103/PhysRevB.95.184412, url = https://link.aps.org/doi/10.1103/PhysRevB.95.184412,” .
- [77] Y. Mizuno, T. Tohyama, S. Maekawa, T. Osafune, N. Motoyama, H. Eisaki, and S. Uchida, “Electronic states and magnetic properties of edge-sharing Cu-O chains,” *Phys. Rev. B* **57**, 5326–5335 (1998).
- [78] Harald Jeschke, Ingo Opahle, Hem Kandpal, Roser Valentí, Hena Das, Tanusri Saha-Dasgupta, Oleg Janson, Helge Rosner, Andreas Brühl, Bernd Wolf, Michael Lang, Johannes Richter, Shijie Hu, Xiaoqun Wang, Robert Peters, Thomas Pruschke, and Andreas Honecker, “Multistep Approach to Microscopic Models for Frustrated Quantum Magnets: The Case of the Natural Mineral Azurite,” *Phys. Rev. Lett.* **106**, 217201 (2011).
- [79] Masayoshi Fujihala, Hiroko Koorikawa, Setsuo Mitsuda, Katsuhiko Morita, Takami Tohyama, Keisuke Tomiyasu, Akihiro Koda, Hirotaka Okabe, Shinichi Itoh, Tetsuya Yokoo, Soshi Ibuka, Makoto Tadokoro, Masaki Itoh, Hajime Sagayama, Reiji Kumai, and Youichi Murakami, “Possible Tomonaga-Luttinger spin liquid state in the spin-1/2 inequilateral diamond-chain compound $\text{K}_3\text{Cu}_3\text{AlO}_2(\text{SO}_4)_4$,” *Sci. Rep.* **7**, 16785 (2017).
- [80] Guillaume Radtke, Andrés Saúl, Hanna A. Dabkowska, Myron B. Salamon, and Marcelo Jaime, “Magnetic nanopantograph in the $\text{SrCu}_2(\text{BO}_3)_2$ Shastri–Sutherland lattice,” *PNAS* **112**, 1971–1976 (2015).
- [81] Sebastian Paeckel, Thomas Khler, Andreas Swoboda, Salvatore R. Manmana, Ulrich Schollwck, and Claudius Hubig, “Time-evolution methods for matrix-product states,” *Ann. Phys.* **411**, 167998 (2019).